XV International Conference on Computational Plasticity. Fundamentals and Applications
COMPLAS 2019
E. Oñate, D.R.J. Owen, D. Peric , M. Chiumenti, and Eduardo de Souza Neto (Eds)

ZERO-THICKNESS INTERFACE MODEL WITH CHEMICAL DEGRADATION BY ACID ATTACK

A. MARTÍNEZ, J. LIAUDAT, C. M. LÓPEZ AND I. CAROL

School of Civil Engineering (ETSECCPB)
Universitat Politècnica de Catalunya (UPC)
Campus Nord UPC, 08034 Barcelona, Spain
e-mail: ariadna.martinez.e@upc.edu, joaquin.liaudat@upc.edu, carlos.maria.lopez@upc.edu, ignacio.carol@upc.edu

Key words: oil-well cement, acid attack, CO_2, interface elements, constitutive law, C-M coupling

Abstract. Carbon dioxide (CO_2) storage in abandoned oil/gas reservoirs is considered a viable alternative to reduce greenhouse gas emissions to the atmosphere. An important element of the risk associated with long-term CO_2 storage is the loss of integrity of the cement seals of the abandoned wells in the reservoir. Among others, one possible cause of loss of integrity is the degradation of the oil-well cement due to the acid attack of the carbonated brine in the reservoir. In previous studies, the authors have developed a diffusion-reaction model for simulating this degradation process. In order to study possible coupled Chemo-Mechanical (C-M) mechanisms, this model will be coupled with an existing mechanical model. For this purpose, in this paper, an existing constitutive law for zero-thickness interface, based on the theory of elasto-plasticity with concepts of fracture mechanics, is modified to incorporate the effect of chemical degradation on the mechanical strength parameters. Preliminary results obtained with this new constitutive law are presented, in order to illustrate the main aspects of the proposed constitutive law, as well as a possible C-M degradation mechanism that should be considered in the long-term safety assessment of CO_2 geological storage projects.

1 INTRODUCTION

Carbon dioxide (CO_2) storage in depleted oil/gas reservoirs is considered a viable alternative to reduce greenhouse gas emissions to the atmosphere. One of the major sources of concern with this type of projects is the presence of abandoned wells which perforate the caprock of the reservoir and which may potentially constitute CO_2 leakage pathways. In many cases, the plugging of abandoned wells began decades ago when CO_2 storage was not under consideration and, therefore, the primary cement used for the casing and/or the plug cement in the well were regular Portland cements (e.g. API Class G and H oilwell cement). These cements, which are basic in nature, are chemically unstable in acidic environments as the one resulting from the injection of CO_2 into the reservoir [1–6].

The CO_2 injected progressively dissolves in the water or brine filling the depleted reservoir, leading to the formation of carbonic acid, with a consequent decrease of the pH. As the carbonated brine reaches the oil-well cement, a number of chemical reactions occur between

the aqueous carbon species and the Hydrated Cement Paste (HCP). These reactions combined with the diffusion of aqueous species in the HCP pore solution leads to the development of a decalcification front, which advances into the material. In the decalcified zones of the HCP, only an amorphous silica gel remains, which shows practically no mechanical strength and very high permeability [7]. A detailed discussion of this chemical degradation process may be found in Ref. [8].

The velocity of advancement of the degradation front is relatively slow (a few millimetres per month) and decreases as the degradation front moves into the HCP [3, 6]. If compared with typical well cementation lengths of tens of meters, the advancement of the degradation front *per se* does not seem to have the potential of compromising the integrity of the well seals. However, if the acid attack is considered in combination with the mechanical loads acting on the well cement in the reservoir, the picture could be different.

The time evolution of the pore pressure in the reservoir because of the injection/extraction of fluids, combined with the fact that well cementing is done in different times of the well life, may induce significant stresses on the well cement, including tensile stresses [9]. These stresses may induce the propagation of cracks, in particular in the interfaces between the cement and the steel case and between the cement and the rock. If the carbonated brine penetrates these cracks, the strength reduction due to the acid attack of the crack tip may induce subcritical crack growth with consequent risk for the integrity of the well.

In order to study this Chemo-Mechanical (C-M) degradation mechanism, a numerical model is being developed by the authors in the context of an ongoing research project. For this purpose, a diffusion-reaction model for simulating acid attack on oil-well cements exposed to carbonated brine, recently developed by the authors [8, 10, 11], will be coupled with an existing mechanical model. This mechanical model has the characteristic ingredient of using zero-thickness interface elements with double nodes for representing cracks, e.g. [12-14]. As a necessary intermediate step, in this paper, a new constitutive law for the interface elements is briefly described which makes it possible to incorporate the effect of degradation of the mechanical strength by the acid attack. This constitutive law is obtained by modifying an existing one based on the theory of elasto-plasticity, with concepts and parameters from the non-linear fracture mechanics theory [12-14]. Preliminary results obtained with this new constitutive law are presented, in order to illustrate the main aspect of the new constitutive law, as well as coupled C-M degradation mechanisms that should be considered in the long-term safety assessment of CO_2 geological storage projects.

2 CONSTITUTIVE LAW FOR ZERO-THICKNESS INTERFACE ELEMENTS WITH CHEMICAL DEGRADATION

The constitutive law is formulated in terms of the normal and tangential stress components in the mid-plane of the interface element $\boldsymbol{\sigma} = [\sigma_N, \sigma_T]^{\mathrm{t}}$ and the conjugate relative displacements $\mathbf{u} = [u_N, u_T]^{\mathrm{t}}$ ($^{\mathrm{t}}$ = transposed). The law is based on the theory of elasto-plasticity and introduces nonlinear fracture mechanics concepts in order to define the softening behaviour due to the work dissipated in the fracture process (denoted W^{cr}).

The fracture surface $F(\boldsymbol{\sigma}) = 0$ is defined by a hyperbola of three parameters (Fig. 1a):

$$F(\boldsymbol{\sigma}) = -(c - \sigma_N \tan\phi) + \sqrt{\sigma_T^2 + (c - \chi \tan\phi)^2} = 0 \tag{1}$$

where χ is the tensile strength, c is the apparent cohesion, and ϕ is the asymptotic friction angle. Cracking starts when the fracture surface is reached. As the fracture process and/or the chemical degradation progress, the fracture surface shrinks. In order to control the evolution process of the fracture surface, the model incorporates two parameters, G_F^I and G_F^{IIa}, that represent the specific fracture energy in Mode I and in Mode II under high confinement, respectively (Fig. 1b). These two parameters are reduced by the chemical degradation of the material. Total exhaustion of tensile strength ($\chi = 0$) is reached either for $W^{cr} = G_F^I$ or for $\eta = 1$ (curve "1" in Fig. 1c), and residual frictional strength ($c = 0$ and $\tan\phi = \tan\phi_r$) is obtained for $W^{cr} = G_F^{IIa}$ (curve "2" in Fig. 1c).

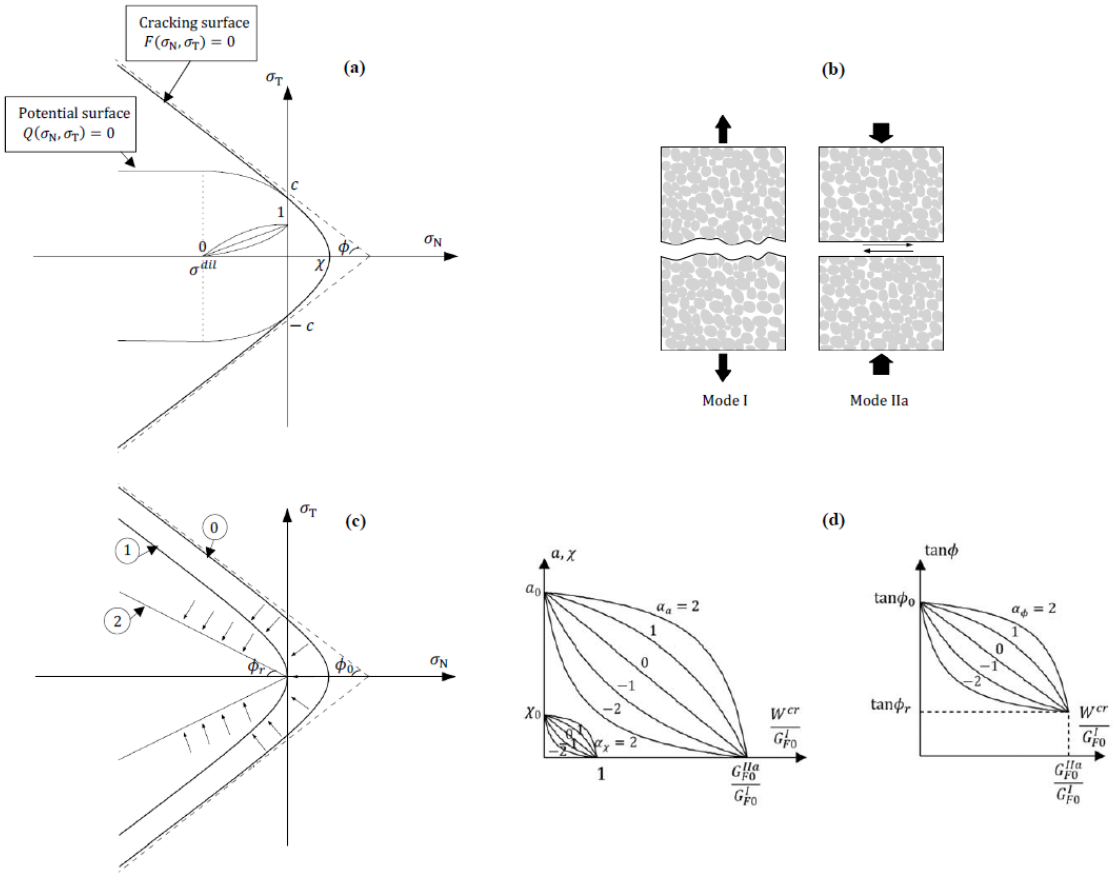

Figure 1: Crack laws for material without chemical degradation ($\eta = 0$): (a) cracking surface and potential surface; (b) fundamental modes of fracture; (c) evolution of cracking surface; (d) softening laws for χ, a, and $\tan\phi$. Adapted from [12, 14].

The work spent on the fracture process during the formation of the crack is given by:

$$\begin{aligned} dW^{cr} &= \sigma_N\, du_N^{cr} + \sigma_T\, du_T^{cr} \qquad \text{if } \sigma_N \geq 0 \\ dW^{cr} &= \sigma_T\, du_T^{cr} \left(1 - \left|\frac{\sigma_N \tan\phi}{\sigma_T}\right|\right) \quad \text{if } \sigma_N < 0 \end{aligned} \tag{2}$$

These expressions imply that, in tension, all work dissipated in the crack goes into the fracture process, while, in compression, the contribution of W^{cr} comes only from the shear work by subtracting the basic friction.

The parameters of the fracture surface evolve by means of the following softening laws:

$$\chi = \chi_0[1 - S(\xi_\chi)][1 - S(\eta)] \tag{3}$$

$$\tan\phi = \tan\phi_0[1 - S(\xi_\phi)] + \tan\phi_r\, S(\xi_\phi) \tag{4}$$

$$a = a_0[1 - S(\xi_a)] \tag{5}$$

where ξ_χ, ξ_ϕ, and ξ_a are dimensionless positive internal variables which grow with W^{cr}, η is the dimensionless history variable representing the chemical degradation of the material ($\eta = 0$ for non-degraded material, $\eta = 1$ for completely degraded material). $S(X)$ is a scaling function which makes it possible to obtain a family of evolution curves for different values of the shape parameter α (Fig. 1d). The variable a is the horizontal distance between the vertex of the updated hyperbola and its asymptotes, in such a way that the updated apparent cohesion c is obtained from the following expression:

$$c = (a + \chi)\tan\phi \tag{6}$$

The internal variable ξ_χ is defined in a differential form as follows:

$$d\xi_\chi = \frac{dW^{cr}}{G_F^I(\eta)} \tag{7}$$

The specific fracture energy in Mode I evolves with η according to:

$$G_F^I(\eta) = G_{F_0}^I[1 - S(\eta)] + G_{Fmin}^I\, S(\eta) \tag{8}$$

where $G_{F_0}^I$ and G_{Fmin}^I are the values of G_F^I for $\eta = 0$ (non-degraded material) and $\eta = 1$ (completely degraded material), respectively.

Similarly, the internal variables ξ_ϕ and ξ_a are given by:

$$d\xi_\phi = d\xi_a = \frac{dW^{cr}}{G_F^{IIa}(\eta)} \tag{9}$$

Assuming that the ratio $G_F^{IIa}(\eta)/G_F^I(\eta)$ remains constant for any value of η, the following relationship is obtained from Eqs. (7) and (9):

$$\xi_\phi = \xi_a = \xi_\chi \frac{G_{F0}^I}{G_{F0}^{IIa}} \tag{10}$$

Note that the effect of the increasing chemical degradation (increasing η) on the mechanical strength of the material is considered in two ways: (i) by reducing the tensile strength (Eq. (3)), and (ii) by reducing the specific fracture energies G_F^I and G_F^{IIa} (Eq. (8)).

3 PRELIMINARY RESULTS

In the following sections, a number of simple academic examples are presented in order to illustrate the main features of the proposed constitutive law. In these examples, three different mechanical loading schemes (pure tension, shear under compression, and three-point bending) are considered combined with chemical degradation.

3.1 Pure tension tests

The pure tension tests are simulated considering a single zero-thickness interface element with the following parameters: $K_N = K_T = 100000$ MPa/mm, $\chi_0 = 3$ MPa, $c_0 = 7$ MPa, $G_{F0}^I = 0.03$ N/mm, $G_{F0}^{IIa} = 10G_{F0}^I$, and $G_{Fmin}^I = 0.01G_{F0}^I$. The results obtained for different sequences ("cases") of loading and chemical degradation are shown in Figs. 2–4. In those figures, Case 0 is the reference case corresponding to an interface element subjected to increasing normal relative displacement, without any chemical degradation. Note that because the adopted chemical degradation rates are arbitrary, time is given as a dimensionless variable.

In Cases 1 and 2 (Fig. 2), an initial normal relative displacement (u_N) is imposed until reaching the initial tensile strength of the interface (χ_0). Thereafter, u_N is progressively increased together with the chemical degradation parameter (η), with higher degradation rate for Case 2 than for Case 1. It can be appreciated that a higher rate of chemical degradation implies a faster decrease of the tensile strength of the interface element.

In Case 3 (Fig. 2), an initial u_N is also imposed, but without surpassing the tensile strength. This initial u_N is kept constant while the chemical degradation is increased until $\eta = 0.6$. According with Eq. (3), this leads to a reduction of the tensile strength with consequent cracking (plastification) of the interface element. Thereafter, u_N is progressively increased without additional chemical degradation.

In Cases 4 and 5 (Fig. 3), an initial u_N is imposed which cracks (plastifies) the interface. This initial u_N is kept constant while η is progressively increased, with a different rate in each case. The chemical degradation decreases the normal stress in the interface due to the contraction of the fracture surface. As expected, the higher the chemical degradation rate, the higher the decrease of the normal stress. Thereafter, u_N is progressively increased without additional chemical degradation.

In Cases 6 and 7 (Fig. 4), the same sequences of mechanical and chemical degradation as in Cases 4 and 5 are followed, with the only difference that now the interface elements are partially unloaded before applying the chemical degradation. Note that because K_N is very high, the unloading of the interface implies practically no change in u_N. As expected, the softening branch obtained for Cases 6 and 7 are exactly the same as for Cases 4 and 5, respectively.

3.2 Shear under compression tests

The tests with shear under compression loading are also simulated considering a single interface element, and with the same parameters as in the previous examples. The results obtained for different sequences of loading and chemical degradation are shown in Figs. 5–7. In those figures, Case 0 is the reference case corresponding to an interface element subjected to increasing tangential relative displacement (u_T), without any chemical degradation. A constant normal stress $\sigma_N = -2$ MPa is considered in all cases.

In Case 1 (Fig. 5), an initial u_T is imposed reaching the initial shear strength of the interface (point a). Then, u_T is progressively increased together with the chemical degradation parameter (η).

In Case 2 (Fig. 5), an initial u_T is imposed in the elastic range of the interface (point b). This initial u_T is kept constant while η is increased until reaching complete chemical degradation ($\eta = 1$). Then, u_T is further increased until reaching the residual frictional strength. Note that at point c, the tensile strength of the interface is null ($\chi = 0$), but the shear strength is not completely degraded yet.

In Cases 3 and 4 (Fig. 6), different initial u_T are imposed, which crack the interface element. In Case 3, the work spent in the fracture process (W^{cr}) due to the imposed u_T is lower than the specific fracture energy in mode I, i.e. $W^{cr} < G_{F0}^{I}$, while in Case 4, the initial u_T is such that $W^{cr} > G_{F0}^{I}$. In both cases, the initial u_T is kept constant while η is increased until reaching $\eta = 0.6$. Thereafter, in both cases, u_T is increased without additional chemical degradation. Note that, in both cases, as u_T is increased, the shear strengths tend to the residual frictional strength.

In Cases 5 and 6 (Fig. 7), the same sequences of mechanical and chemical degradation as in Cases 3 and 4 are followed, with the only difference that now the interface elements are partially unloaded before applying the chemical degradation. As expected, the softening branch obtained for Cases 5 and 6 are exactly the same as for Cases 3 and 4, respectively.

3.3 Three-point bending test

This example is intended to simulate the propagation of an initially stable flexural crack in a beam due to the chemical degradation of the tip of the crack. For this purpose, a two-dimensional (plane stress) beam of 0.6 m length and 0.1 m height is considered, with a line of interface elements in the central section (Fig. 8). The continuum elements are assumed linear elastic ($E = 25000$ MPa, $\nu = 0.2$) and the interface elements are equipped with the constitutive law presented in this paper, with the same parameters as for the other examples.

It is considered that the chemical degradation rate is the same at all the integration points of the interface elements, but that it only starts if the integration point has been cracked ($W^{cr} > 0$). This latter assumption is made in order to mimic, in a very simplified manner, the C-M mechanism described in the Introduction, in which the ingress of carbonated brine in pre-existing cracks in the well cement may lead to sub-critical grow due to the acid attack of the tip of the crack.

The beam is initially loaded with a negative vertical displacement which is applied at mid-span, on the upper face of the beam, until the first interface element from the lower face of the beam starts to crack. This initial vertical displacement is kept constant until the end of the test. The deformed mesh and the normal stresses in the interface elements corresponding to this initial condition are indicated with time t = 0 in Fig. 8. In this condition, the chemical degradation starts in the first interface element, leading to the contraction of the fracture (plastic) surface and the consequent reduction of the tensile strength (χ). This reduction of the tensile strength of the first interface element leads to a stress redistribution, which increases the normal stresses in the interface elements above it. Eventually, this stress redistribution causes the cracking of the second interface element, triggering its chemical degradation. As time goes by, this process progresses leading to the propagation of the initial crack, as it is shown in Fig. 8.

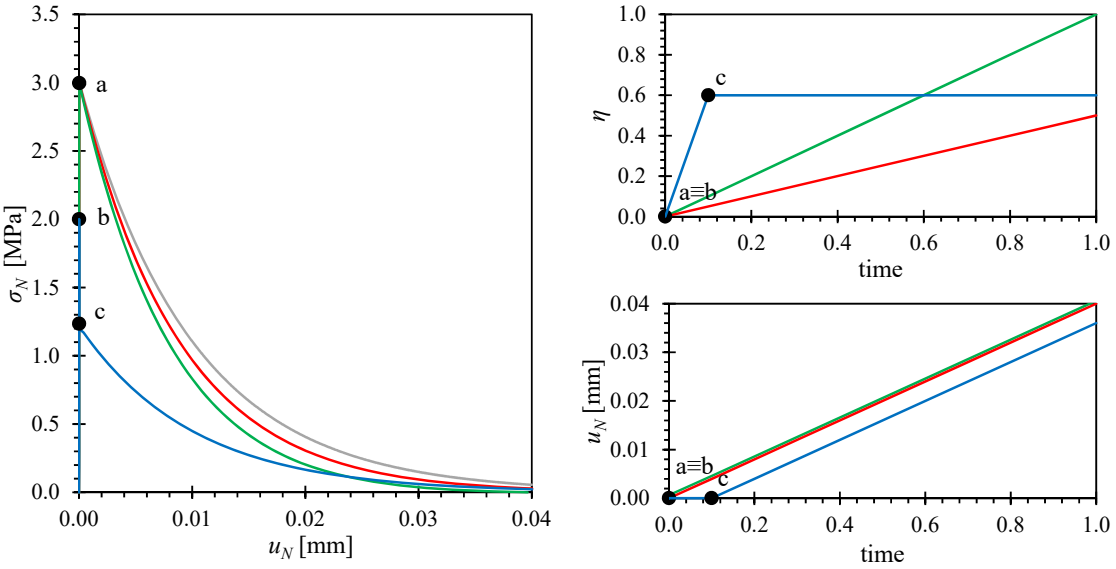

Figure 2: Pure tension tests combined with different cases of chemical degradation described in the body of the text: Case 0 (grey line), Case 1 (red lines), Case 2 (green lines), and Case 3 (blue lines). Left plot, normal stress versus normal relative displacement. Upper-right plot, chemical degradation versus time. Lower-right plot, normal relative aperture versus time. The red line in the lower-right plot has been slightly shifted for the sake of clarity.

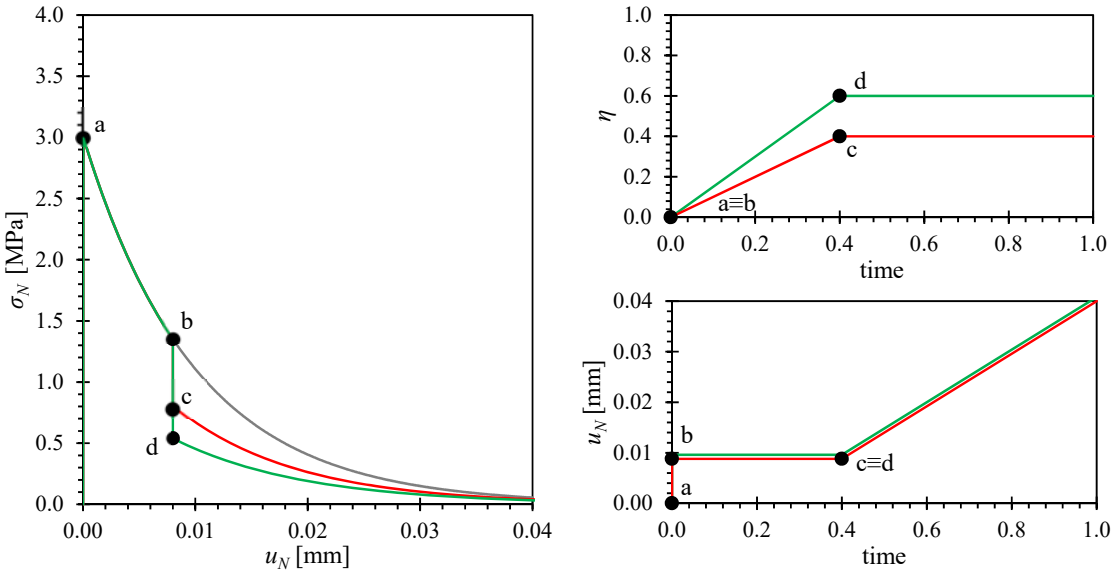

Figure 3: Pure tension tests combined with different cases of chemical degradation described in the body of the text: Case 0 (grey line), Case 4 (red lines), and Case 5 (green lines). Left plot, normal stress versus normal relative displacement. Upper-right plot, chemical degradation versus time. Lower-right plot, normal relative aperture versus time. The green line in the lower-right plot has been slightly shifted for the sake of clarity.

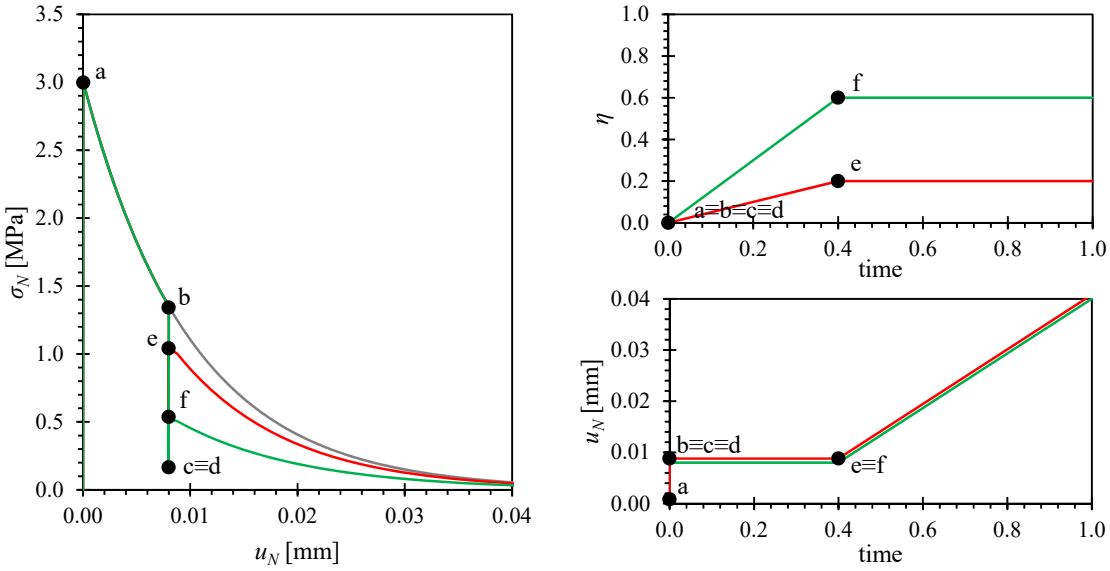

Figure 4: Pure tension tests combined with different cases of chemical degradation described in the body of the text: Case 0 (grey line), Case 6 (red lines), and Case 7 (green lines). Left plot, normal stress versus normal relative displacement. Upper-right plot, chemical degradation versus time. Lower-right plot, normal relative aperture versus time. The green line in the lower-right plot has been slightly shifted for the sake of clarity.

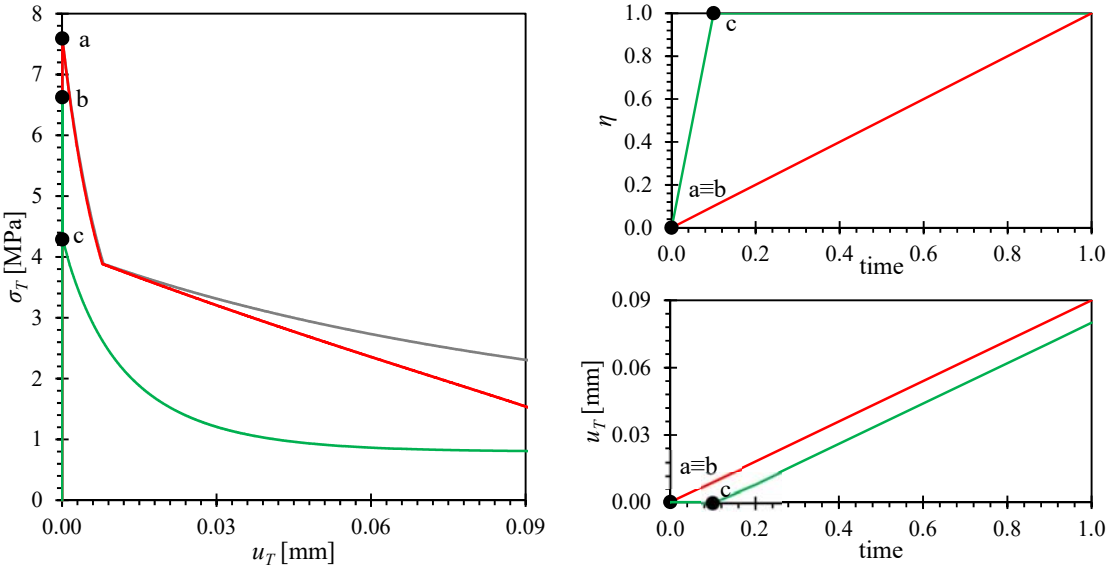

Figure 5: Shear under compression tests combined with different cases of chemical degradation described in the body of the text: Case 0 (grey line), Case 1 (red lines), and Case 2 (green lines). Left plot, normal stress versus normal relative displacement. Upper-right plot, chemical degradation versus time.

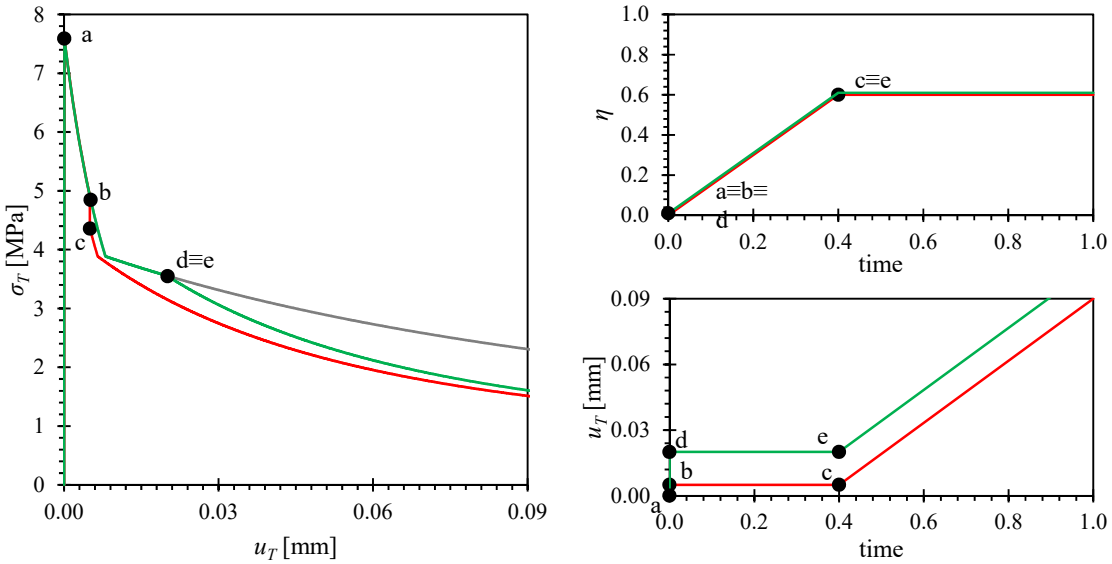

Figure 6: Shear under compression tests combined with different cases of chemical degradation described in the body of the text: Case 0 (grey line), Case 3 (red lines), and Case 4 (green lines). Left plot, normal stress versus normal relative displacement. Upper-right plot, chemical degradation versus time. The green line in the upper-right plot has been slightly shifted for the sake of clarity.

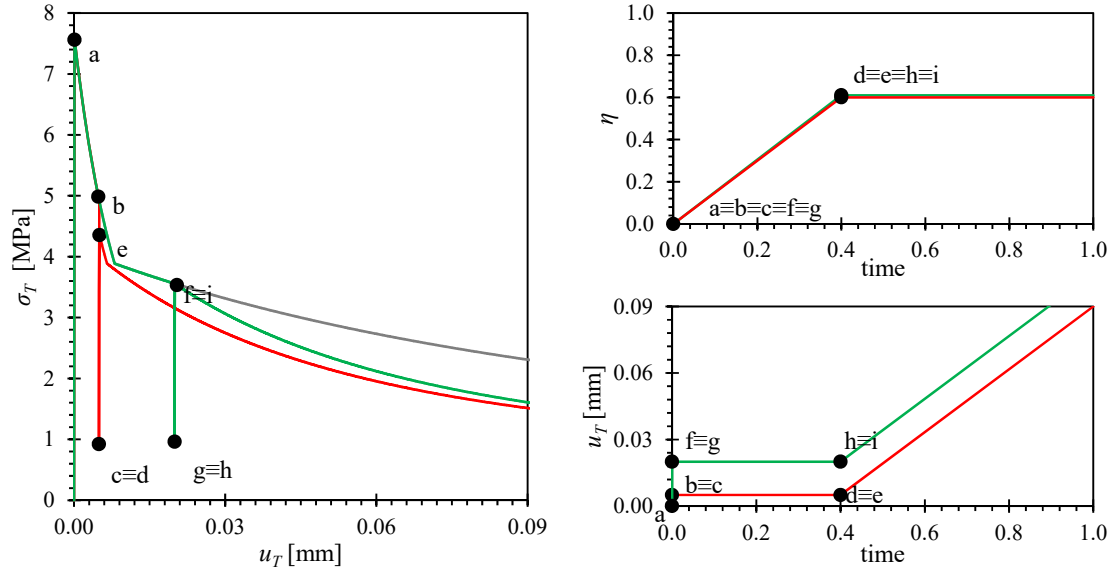

Figure 7: Shear under compression tests combined with different cases of chemical degradation described in the body of the text: Case 0 (grey line), Case 5 (red lines), and Case 5 (green lines). Left plot, normal stress versus normal relative displacement. Upper-right plot, chemical degradation versus time. The green line in the upper-right plot has been slightly shifted for the sake of clarity.

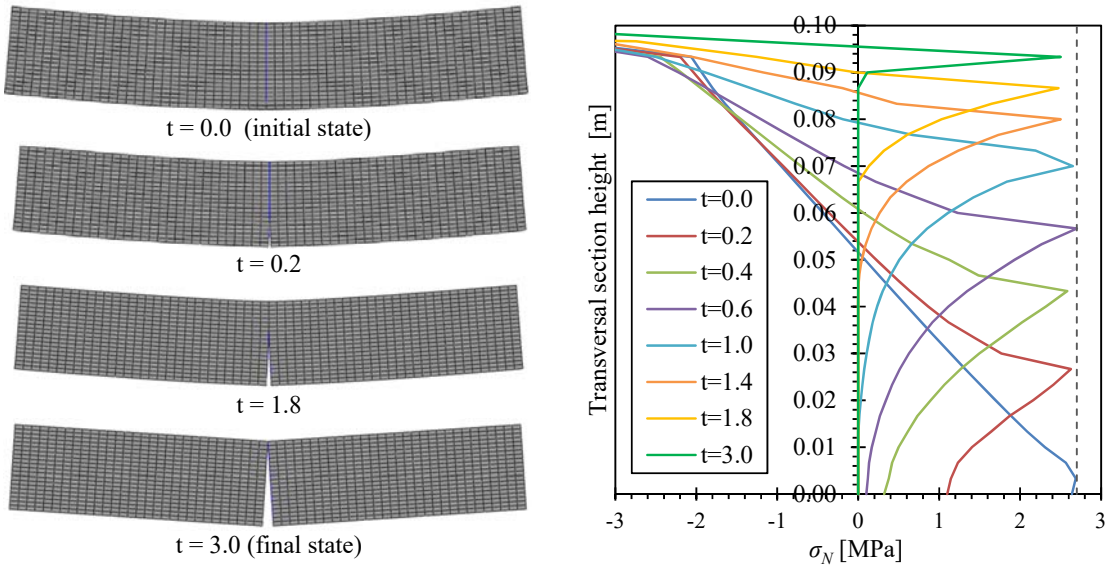

Figure 8: Three-point bending test. An initial vertical displacement is imposed to the mid-span point of the upper face of the beam, and it is kept constant while the chemical degradation of the cracked interface elements makes the flexural crack to grow. Left, deformed FE mesh (× 200) at different times. Right, time evolution of the normal stress profile of the central section of the beam as the fracture progresses due to the chemical degradation.

4 CONCLUDING REMARKS

- A C-M mechanism which may lead to the propagation of cracks in oil-well cements exposed to carbonated brines is proposed.
- In order to reproduce this mechanism with a coupled FE C-M model, a new constitutive law for zero-thickness interface elements is being developed.
- This constitutive law makes it possible to simulate the reduction of the material strength parameters due to chemical degradation processes, such as acid attack of oilwell cements.
- The behaviour of the new law is illustrated by a number of simple academic tests, including pure tensile tests, shear under compression tests, and a three-point bending test.
- The preliminary results obtained seem indicate that the proposed C-M mechanism for sub-critical crack propagation due to acid attack can be simulated with the new constitutive law.

ACKNOWLEDGMENTS

This research has been supported by MEC (Madrid) through project BIA2016-76543-R, which includes European FEDER funds, and 2017SGR-1153 from Generalitat de Catalunya (Barcelona). The first author also acknowledges AGAUR (Barcelona) for her FI doctoral fellowship.

REFERENCES

[1] Gasda, S.E., S. Bachu and M.A. Celia. The potential for CO_2 leakage from storage sites in geological media: analysis of well distribution in mature sedimentary basins. *Environmental Geology* (2004) **46**(6–7):707–720.

[2] Kutchko, B.G., Strazisar, B.R., Dzombak, D.A., Lowry, G.V., Thaulow, N. Degradation of well cement by CO_2 under geologic sequestration conditions. *Environmental Science and Technology* (2007) **41**:4787–4792.

[3] Kutchko, B.G., Strazisar, B.R., Lowry, G.V., Dzombak, D.A., Thaulow, N. Rate of CO_2 Attack on Hydrated Class H Well Cement under Geologic Sequestration Conditions. *Environmental Science and Technology* (2008) **42**:6237–6242.

[4] Rimmelé, G., Barlet-Gouédard, V., Porcherie, O., Goffé, B., Brunet, F. Heterogeneous porosity distribution in Portland cement exposed to CO_2-rich fluids. *Cement and Concrete Research* (2008) **38**:1038–1048.

[5] Carey, J.W., Wigand, M., Chipera, S.J., WoldeGabriel, G., Pawar, R., Lichtner, P.C., Wehner, S.C., Raines, M.A., Guthrie, G.D. Analysis and performance of oil well cement with 30 years of CO_2 exposure from SACROC Unit, West Texas, USA. *International Journal of Greenhouse Gas Control* (2007) **1**:75–85.

[6] Duguid, A., Scherer, G.W. Degradation of oilwell cement due to exposure to carbonated brine. *International Journal of Greenhouse Gas Control* (2010) **4**:546–560.

[7] Duguid, A., Radonjic, M., Scherer, G.W. Degradation of cement at the reservoir/cement interface from exposure to carbonated brine. *International Journal of Greenhouse Gas Control* (2011) **5**:1413–1428.

[8] Liaudat, J., Martínez, A., López, C.M., Carol, I. 2018. Modelling acid attack of oilwell cement exposed to carbonated brine. *International Journal of Greenhouse Gas Control* (2018) **68**:191–202.

[9] Mainguy, M., Longuemare, P., Audibert, A., Lécolier, E. Analyzing the risk of well plug failure after abandonment. *Oil & Gas Science and Technology-Revue de l'IFP* (2007) **62**(3):311-324.

[10] Martínez, A., Liaudat, J., López, C.M., Carol, I. Diffusion-reaction modelling of degradation of oil-well cement exposed to carbonated brine. In *Computational Plasticity XIV - Fundamentals and Applications*, pp.625–635, CIMNE, Barcelona, 2017.

[11] Barandiarán, L., Liaudat, J., López, C.M., Carol, I. Modelling acid attack of oilwell cement exposed to carbonated brine: effect of specimen geometry on experimental results. Submitted to the *XV International Conference on Computational Plasticity - Fundamentals and Applications (COMPLAS XV)*, Barcelona, 2019.

[12] Carol, I, Prat, P.C., López, C.M., A normal/shear cracking model. Application to discrete crack analysis. *Journal of Engineering Mechanics* (1997) **123**(8):765–73.

[13] Carol, I., López, C.M., Roa, O. Micromechanical analysis of quasi-brittle materials using fracture-based interface elements. *International Journal for Numerical Methods in Engineering* (2001) **52**(1-2):193–215.

[14] López, C.M., Carol, I., Aguado, A. Meso-structural study of concrete fracture using interface elements. I: numerical model and tensile behavior. *Materials and structures* (2008) **41**(3):583–599.